Morphology of collisional nonlinear spectra in H2-Kr and H2-Xe mixtures

Waldemar Glaz, Tadeusz Bancewicz, Jean-Luc Godet, George Maroulis, Anastasios Haskopoulos

Morphology of collisional nonlinear spectra in H2-Kr and H2-Xe mixtures

Waldemar Głaz, Tadeusz Bancewicz, Jean-Luc Godet, George Maroulis, and Anastasios Haskopoulos

Citation: The Journal of Chemical Physics **138**, 124307 (2013); doi: 10.1063/1.4795438
View online: http://dx.doi.org/10.1063/1.4795438
View Table of Contents: http://scitation.aip.org/content/aip/journal/jcp/138/12?ver=pdfcov
Published by the AIP Publishing

Morphology of collisional nonlinear spectra in H_2-Kr and H_2-Xe mixtures

Waldemar Głaz,[1,a)] Tadeusz Bancewicz,[1,a)] Jean-Luc Godet,[2,b)] George Maroulis,[3,c)] and Anastasios Haskopoulos[3]
[1]*Nonlinear Optics Division, Faculty of Physics, Adam Mickiewicz University, Umultowska 85, 61-614 Poznań, Poland*
[2]*Laboratoire de Photonique d'Angers, EA 4464, Université d'Angers, 2 boulevard Lavoisier, 49045 Angers Cedex 01, France*
[3]*Department of Chemistry, University of Patras, GR-26500 Patras, Greece*

(Received 11 December 2012; accepted 1 March 2013; published online 26 March 2013)

This article reports new results of theoretical and numerical studies of spectral features of the collision-induced hyper-Rayleigh light scattered in dihydrogen-noble gas (H_2-Rg) mixtures. The most massive and polarizable scattering supermolecules with Rg = Kr and Xe have been added to the previously considered systems in order to gain a more complete insight into the evolution of the spectral properties. The symmetry adapted components of the first collisional hyperpolarizabilities are obtained by means of the quantum chemistry numerical routines supplemented with appropriate theoretical methods. Roto-translational spectral lines are calculated on the grounds of the quantum-mechanical as well as semi-classical approach. The role of particular hyperpolarizability components in forming the line shapes is discussed. The intensities of the lines are compared with those obtained for less massive scatterers. Advantages of prospective application of the new scattering systems for experimental detection of the nonlinear collisional effects are indicated. © *2013 American Institute of Physics*. [http://dx.doi.org/10.1063/1.4795438]

I. INTRODUCTION

Intermolecular interactions and related phenomena in which the hydrogen molecule is involved are currently of interest because of their importance to astrophysics, atmospheric research as well as for molecular physics, chemistry, and biology. On the other hand, technical and industrial applications in this field are also of growing importance. Being the most abundant compound in the universe dihydrogen is relevant to the interpretation of spectroscopic data obtained form observations of distant stellar and planetary objects.[1,2] Additionally, its complexes formed with foreign atomic or molecular units may be invaluable source of data concerning the other entities—their individual or collective features and correlations.[3,4] More practical matters could be also mentioned in this context,[5] including, for instance, physisorption as a potential method for the efficient storage of H_2 or remote sensing techniques.[6] Therefore, it has come as no surprise that in molecular spectroscopy the systems composed of dihydrogen-dihydrogen or dihydrogen-(rare gas atom) pairs have become the compounds of interest for their convenient experimental attainment and relatively straightforward theoretical interpretation of their behavior. For the same reasons they are widely regarded as prototype systems applied for modeling purposes of the properties and interactions of more complex structures.[3,4]

Following these ideas, this report is intended as a continuation of a series of previously published papers on spectral analyses of the hyper-Rayleigh collision-induced light scattering processes (CIHR) in dihydrogen-rare gas (Rg) pairs comprising H_2-He (Ref. 7), H_2-Ne (Ref. 5), and H_2-Ar (Ref. 8) pairs. Some essential features of the interaction in the above pairs have been also explored in some depth, theoretically for H_2-Ar (Refs. 9 and 10) as well as–computationally for H_2-He and H_2-Ne (Refs. 11 and 12); this study is now to be expanded to include the remaining H_2-Rg weakly bound molecules (Rg = Kr and Xe).

The hyper-Rayleigh (HR) light scattering phenomena considered in the earlier works represent nonlinear effects in which the frequency of the incident light is doubled during a three photon scattering event. Its occurrence is attributed to relevant optical quantities characterizing a scatterer (hyper-/polarizabilities) that may be intrinsic features of an individual microscopic entity or transient effects mediated by intermolecular interactions. The hyper-Rayleigh process originates in the Rayleigh first-hyperpolarizability property. This third order tensor, $\mathbf{\Delta}\beta_{ijk}$, is in general symmetric in its last two indexes[13–15] (two fields of laser radiation are indistinguishable). However in transparent media and far from electron resonances to a good approximation this quantity can be considered as fully symmetric in all its indexes.[16] On the basis of this assumption, the third order first-hyperpolarizability tensor is actually a tensorial sum, $\Delta\boldsymbol{\beta} = \Delta\boldsymbol{\beta}^{(1)} \oplus \Delta\boldsymbol{\beta}^{(3)}$, of the irreducible spherical vector and septor part of weight 1 and 3, respectively.[17] Usually, in an analytical description of physical phenomena the vector and septor parts of the hyperpolarizability are not expressed as mixed terms, analogously to the isotropic and anisotropic parts of the linear

a)Authors to whom correspondence should be addressed. Electronic addresses: glaz@amu.edu.pl and tbancewi@zon12.physd.amu.edu.pl. URL: http://zon8.physd.amu.edu.pl/~tbancewi.
b)Electronic mail: jean-luc.godet@univ-angers.fr
c)Electronic mail: maroulis@upatras.gr

polarizability in the linear Rayleigh and Raman light scattering.[18] Therefore, in the present study the vector and septor parts of the collision-induced hyperpolarizability (CIH) tensor are considered separately. Consequently, in spectral computing the vector CIHR spectrum and the septor CIHR spectra are also distinguished from each other.

The monomer hyperpolarizabilities, and the nonlinear radiative effects they bring about, have been extensively studied both theoretically[15,19–22] and experimentally,[23–26] while a method of analysis of the collisional phenomena is still to be developed. Significant work has been reported on the H_2-Kr/Xe systems. Kudian and Welsh[27] have analyzed the spectra of both supermolecules in pressure-induced infrared absorption. Anisotropic intermolecular force effects in similar spectra have been obtained for H_2-Kr, H_2-Xe and D_2-Kr, D_2-Xe by McKellar and Welsh.[28] Dunker and Gordon[29] analyzed the spectra of both complexes to obtain anisotropic intermolecular potentials and transition dipole moments. The collision-induced absorption spectra of D_2 in mixtures of D_2-Kr have been observed by Abu-Kharma *et al.*[30]

The organization of the paper reflect the initial motivation of the study: to develop a thorough theoretical description of CIHR spectral properties induced in mixtures of dihydrogen and the heaviest noble gas atoms with addition efforts aimed at an assessment of experimental feasibility of detecting this effect. To this end, in Sec. II the basic concepts and details of computing procedures regarding the collision-induced hyperpolarizabilities are given: the methods of determining the symmetry adapted components are briefly described and the *ab initio* quantum chemistry (QC) algorithms are discussed. Section III is devoted to theoretical and numerical techniques that have been used for evaluating roto-translational CIHR spectra. Exemplary CIH functional shapes and spectral CIHR profiles are illustrated in figures of Sec. IV and discussed. Experimental aspects are also considered in this section.

II. HYPERPOLARIZABILITIES

A. *Ab initio* calculation of the interaction-induced hyperpolarizability

The calculation of the interaction-induced electric properties of the H_2-Kr and H_2-Xe pairs leans heavily on the experience accumulated from the previous work on such systems as H_2-H_2, Ne-HF, Ne-FH, and Rg-Rg (Rg = He, Ne, Ar, and Kr),[31] Rg-CO_2 (Rg = He, Ne, Ar, Kr, and Xe),[32] Ne-Ar (Refs. 33 and 34), Xe-Xe (Refs. 35), Kr-Xe (Refs. 36 and 37), and H_2O-Rg (Rg = He, Ne, Ar, Kr, and Xe).[11] Only a few essentials are given here.

The interaction-induced properties for a pair consisting of subunits **A** and **B** are extracted from calculations on the **A-B** supermolecules. Basis set superposition error (BSSE) effects are removed by the counterpoise (CP) method of Boys and Bernardi.[38] All relevant calculations are performed with the CCSD method, single and double excitation coupled-cluster theory. All basis sets have been tested in previous work. Atom-specific, purpose oriented basis sets are used for both Kr and Xe. These are Kr = [8*s*7*p*6*d*1*f*] (Ref. 31) and Xe = [9*s*8*p*7*d*1*f*] (Ref. 35). A molecule-specific, purpose oriented [6*s*4*p*3*d*] basis set was used for H_2 (Ref. 31). The bond length of H_2 was kept fixed at 1.449 a_0. To test the quality of the above basis sets we calculated a few basic electric properties at the CCSD level of theory (all electrons correlated). For the two atoms the calculated dipole polarizabilities are $\alpha = 17.16$ (Kr) and 28.11 $e^2a_0^2E_h^{-1}$ (Xe). Both agree quite well with the theoretical estimates proposed by Rice *et al.*[39] For the dipole-dipole-quadrupole hyperpolarizability it is found that B = −328 (Kr) and −786 $e^3a_0^4E_h^{-2}$ (Xe), which is in very good agreement with the earlier values obtained by Maroulis and Thakkar.[40] For H_2 the values of the quadrupole and hexadecapole moments are $\Theta = 0.4791$ ea_0^2 and $\Phi = 0.3645$ ea_0^4. For the dipole polarizability (with z as the molecular axis) the longitudinal and transversal components are $\alpha_{zz} = 6.74$ and $\alpha_{xx} = 4.74$ $e^2a_0^2E_h^{-1}$, respectively. For the components of the dipole-octopole polarizability (E) and the dipole-dipole-quadrupole (B) hyperpolarizability it is obtained that $E_{z,zzz} = 4.38$, $E_{x,xxx} = -1.85$ $e^2a_0^4E_h^{-1}$ and $B_{zz,zz} = -101$, $B_{xz,xz} = -68$, $B_{xx,zz} = 38$, $B_{xx,xx} = -73$ $e^3a_0^4E_h^{-2}$. All the above electric property values agree quite well with the reference data given by Li and Hunt[41] in their work on H_2-H_2. All calculations have been accomplished with the GAUSSIAN 03 program.[42]

B. Collisional symmetry adapted hyperpolarizability components

For a pair composed of a linear centrosymmetric molecule and an atom, such as H_2-Kr and H_2-Xe systems considered in this work, the collision-induced hyperpolarizability tensor $\Delta\boldsymbol{\beta}$ depends on the H_2 molecule orientation $\Omega \equiv (\theta, \varphi)$ and the relative supermolecular spatial arrangement determined by the length and orientation of the vector $\boldsymbol{R}$ connecting the centers of mass of H_2 and Rg.[17,43,44] For this pair the Cartesian reference system (XYZ) is attached with its origin in the center of H_2 molecule. To simplify the considerations, the vector $\boldsymbol{R}$ is chosen to be parallel to the Z axis. The Cartesian components of CIH are computed using the quantum chemistry methods described in Subsection II A[45,46] for three relative H_2-Rg intermolecular geometries: L-shaped ($\theta = 0^\circ$), T-shaped ($\theta = 90^\circ$), and $\theta = 45^\circ$ geometry. Twenty three intermolecular distances, ranging from $R = 4.0$ up to $R = 16.0$ a_0, are taken at each orientation. Next, the transformation from the Cartesian to irreducible spherical tensors $\Delta\beta_\mu^{(K)}(\boldsymbol{R})$ is applied.

To study the rotational behavior of the H_2-Rg pair in respect to the orientational motion of the H_2 molecule and the rotation of $\boldsymbol{R}$ it is convenient to express the vector and the septor part of CI hyperpolarizability $\Delta\boldsymbol{\beta}(R)$ in the form of a linear combination of a properly tailored set of spherical harmonics:[47]

$$\Delta\beta_\mu^{(K)}(\boldsymbol{R}) = \left(\frac{4\pi}{2K+1}\right)^{1/2} \sum_{\lambda L} (2L+1)^{1/2} \times \Delta\beta_{\lambda L}^{(K)}(R)\, Y_{\lambda\mu}(\Omega)\, C_{\lambda\mu L0}^{K\mu}, \quad (1)$$

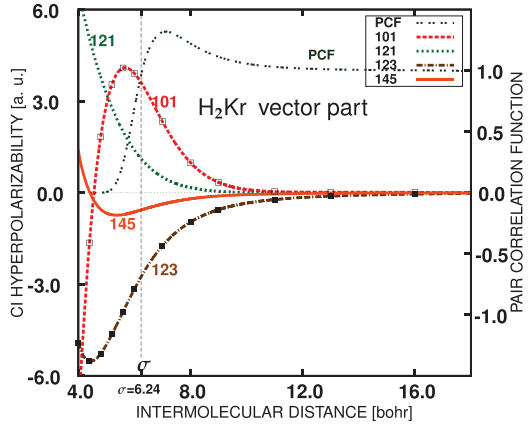

FIG. 1. Collisional symmetry adapted component of the vector part of the hyperpolarizability tensor, $\Delta\beta^{(1)}_{\lambda L}(R)$ (expressed in atomic units); H_2-Kr case. Curves are identified by $K\lambda L$ values. Lines represent analytical functional dependence on intermolecular distance R obtained by fitting to *ab initio* data. Original QC results are indicated as discrete sets of points for two sample profiles. The diameter of collision σ is marked and the pair correlation function illustrated.

with expansion coefficients $\Delta\beta^{(K)}_{\lambda L}(R)$–the so-called symmetry adapted (SA) components of CIH representing the hyperpolarizability dependence on the distance R (Refs. 5 and 47). In Eq. (1) the index K of $\Delta\beta^{(K)}_{\lambda L}(R)$ indicates the rank of the CIH tensor; $K = 1$ for the vector part, $K = 3$ for the septor part, and $C^{K\mu}_{\lambda\mu L0}$ stands for the Clebsch-Gordan coefficient. The rotation of H_2 molecule is related to the index λ, whereas the rotation of $\boldsymbol{R}$ is governed by L. For our configuration the spherical harmonic function $\boldsymbol{R}$ reads as follows: $Y_{Lm}(\hat{\boldsymbol{R}}) = \sqrt{(2L+1)/4\pi}\,\delta_{m0}$.

The symmetry of the system decides which of the irreducible spherical components of CIH are nonzero for particular orientations. For the vector part these are: $\Delta\beta^{(1)}_0(\theta = 0^\circ; R)$, $\Delta\beta^{(1)}_0(\theta = 90^\circ; R)$, $\Delta\beta^{(1)}_0(\theta = 45^\circ; R)$, and $\Delta\beta^{(1)}_1(\theta = 45^\circ; R)$. As a result, a set of four linearly independent equations is derived from the formula in Eq. (1) including four symmetry-adapted components, $\Delta\beta^{(1)}_{01}(R)$, $\Delta\beta^{(1)}_{21}(R)$, $\Delta\beta^{(1)}_{23}(R)$, and $\Delta\beta^{(1)}_{45}(R)$ available for computing.

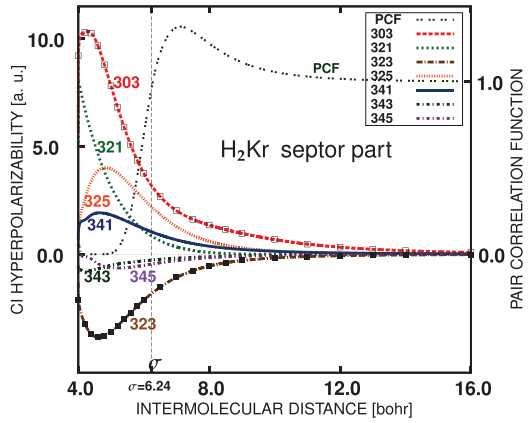

FIG. 2. The same as in Figure 1, though for septor component of H_2-Kr hyperpolarizability.

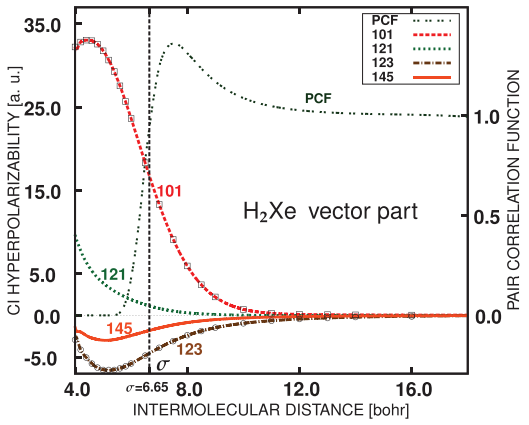

FIG. 3. The same as in Figure 1, though for vector component of H_2-Xe hyperpolarizability.

In the similar manner, the septor case brings forth seven non-vanishing terms: $\Delta\beta^{(3)}_0(\theta = 0^\circ; R)$, $\Delta\beta^{(3)}_{m=0,2}(\theta = 90^\circ; R)$, and $\Delta\beta^{(3)}_{m=0,1,2,3}(\theta = 45^\circ; R)$, which accordingly lead to a set of the same number of equations that can be solved in regard to a specific variety of the SA CIH components: $\Delta\beta^{(3)}_{03}(R)$, $\Delta\beta^{(3)}_{21}(R)$, $\Delta\beta^{(3)}_{23}(R)$, $\Delta\beta^{(3)}_{25}(R)$, $\Delta\beta^{(3)}_{41}(R)$, $\Delta\beta^{(3)}_{43}(R)$, and $\Delta\beta^{(3)}_{45}(R)$. The results are collected in tabular form at http://zon8.physd.amu.edu.pl/~tbancewi. A graphic illustration of the functional dependence represented in the tables is given in Figures 1–4.

III. SPECTRAL AND EXPERIMENTAL CONSIDERATIONS

The method applied in this report and some crucial elements of spectral and experimental analysis resemble to a significant extent those given in the works published before.[5,7,8,48,49] Therefore, only some core points of the procedures are demonstrated hereafter, which—if necessary—can be supplemented by the details provided in the refereed papers.

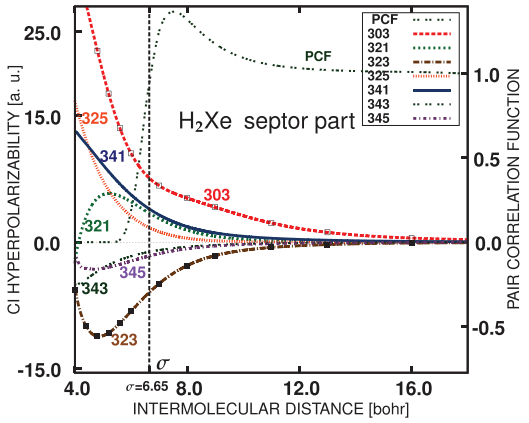

FIG. 4. The same as in Figure 2, though for septor component of H_2-Xe hyperpolarizability.

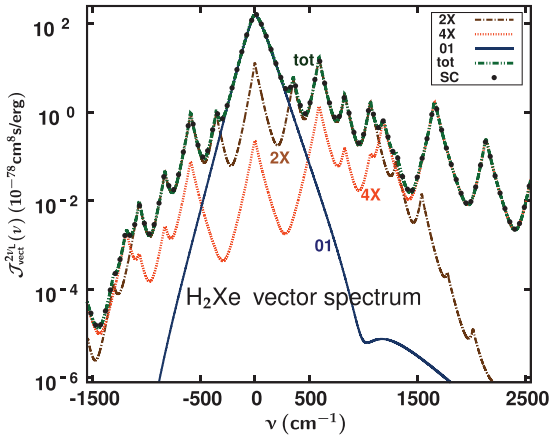

FIG. 5. Roto-translational CIHR spectral profile related to H_2-Xe hyperpolarizability vector part. Solid line depicts total intensity distribution (tot) obtained by quantum-mechanical computations; discrete points show semiclassical (SC) results. Additional shape marked with 01 represents the contribution corresponding to $\lambda L = 01$ symmetry adapted component, while 2X and 4X are overall $\lambda = 2$ and 4 spectral SA shares, respectively.

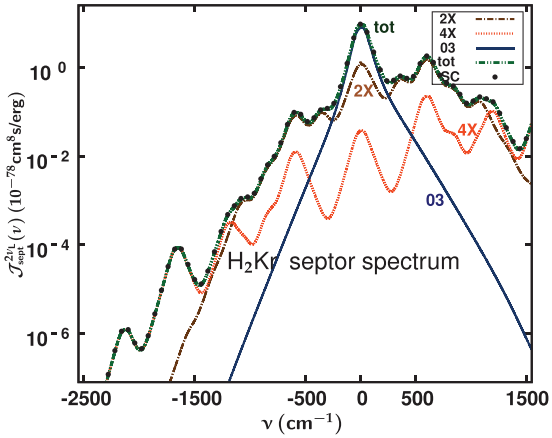

FIG. 6. The same as in Figure 5, yet for the septor CIHR spectrum in H_2-Kr mixture.

A. Theoretical spectra

Most of the relevant data that might be extracted from a HR scattered light beam are conveyed by the translational spectral density profile involved in a convoluted roto-translational (R-T) expression rendering the shape of the experimentally attainable double differential intensity (DDI):

$$\left(\frac{\partial^2 \mathcal{J}^{2\nu_L}}{\partial\,\Omega\,\partial\nu}\right)/\mathcal{J}_0^2 = \frac{\pi}{2\,c}\,k_s^4\,\chi^{(K)}\sum_{\lambda\,L}\sum_{j\,j'}P_j\,(2\,j+1)\,(2\,j'+1) \times \begin{pmatrix} j & \lambda & j' \\ 0 & 0 & 0 \end{pmatrix}^2 g^{(i)}_{\lambda\,L}(\nu-\nu_{jj'}) \qquad (2)$$

where the term of the most significant importance, the translational spectral density $g(\nu - \nu_{jj'})$ is obtained through two independent numerical routines: the quantum mechanical (QM) and semi-classical (SC) approach;[48] a scenario designed for benchmarking purposes of the level of computational accuracy. Within the QM scheme the translational profiles are evaluated by integrating the radial Schrödinger equation on the basis of a modified Numerov algorithm.[48,50] On the other hand, the semi-classical DDI functions are produced by determining classical molecular trajectories dependent on molecular velocities and collisional parameters.[8,51] Subsequently, the Fourier transforms of SA CIH components are yielded by the Posch formulas given in Refs. 52 and 53 and the resulting classical spectra are desymmetrized afterwards in accordance with the *sum rules* values of the semiclassical moments M_0, M_1, and M_2. In both types of the computing routines the intermolecular interactions during collisional encounters are expressed via the potential energy surfaces calculated with reliable codes delivered in works by Roy and co-workers.[54,55] As a result, collisional R-T spectra related to the vector and septor parts of the H_2-Kr and H_2-Xe hyperpolarizabilities are found, of which two exemplary profiles are presented in Figures 5 and 6.

The functional form of DDI represented by Eq. (2) is obtained on the condition that the rotational and translational degrees of freedom are treated independently. This approximate assumption seems justifiable as the first approach solution to the problem, when the influence of intermolecular potential anisotropy is relatively less pronounced. Moreover, such a treatment leads to the DDI expressions in which additive contributions corresponding to a specific set of indices, identifying individual SA hyperpolarizability shares do not mix, hence their influence may be treated and analyzed separately. As a consequence, aggregated lines associated with the SA CIH components labeled λ equal 0, 2, and 4 are singled out and their role is illustrated in the figures mentioned.

B. Experimental remarks

By incorporating the last two heavier supermolecular systems into the family of H_2-Rg compounds of known *ab initio* hyperpolarizability values an opportunity arises of a more complete comparative study of the CIH spatial distribution as well as the spectral properties they determine. It seems rather obvious that the features of CIHR scattering must vary with increasing size of the Rg perturber resulting in more polarizable scattering units. This gives rise to a hope that experimental detection of nonlinear collisional profiles can be more easily achievable. An initial assessment of such a possibility has been undertaken in preceding papers of the series regarding CIHR scattering in the H_2-Ne system, e.g., in Ref. 5.

The quantity that is usually considered as experimentally attainable in nonlinear light scattering measurements is a spectral function that consists of two components related to the vector and septor spectral intensities identified by the index K (K = 1 or 3) in Eq. (2), where the $\chi^{(K)}$ coefficient depends on the geometry of arrangement of the experimental setup used. For instance, for the so-called polarized spectrum, $\mathcal{J}_\perp(\nu)$, $\chi^{(K)}$ is equal 2/9 and 2/21 for K = 1 and 3, respectively.[8] In Figure 7 the R-T polarized intensities are shown for the lighter H_2-Ne systems, considered earlier in this context,[5] and for the van der Waals pairs with Rg = Kr and Xe. In order to estimate feasibility of a realistic experimental treatment of the CIHR spectra, the intensities are usually expressed via counts of photon per second (cps per cm^{-1}). As follows from the analyzes reported in, e.g., Refs. 56 and 57

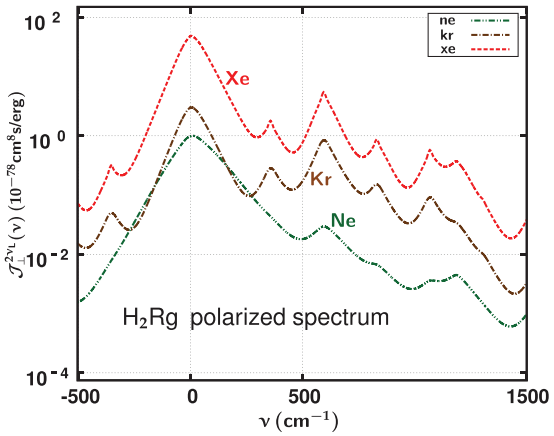

FIG. 7. Evolution of CIHR polarized spectral lines of light scattered by H_2-Rg supermolecules for different Rg scatterers involved (Rg = Ne case from Refs. 5 and 7).

the two quantities are related via the formula:

$$N_f = \frac{2\ln(2)}{hc}\Omega_s n_{H_2} n_{Rg} \frac{r\epsilon_L^2}{\tau}\mathcal{J}(\nu), \tag{3}$$

where the number densities n and parameters characterizing the laser signal properties: r – repetition rate , ϵ – pulse energy, and τ – pulse duration can be changed and adjusted within certain limits according to experimental circumstances and the apparatus sensitivity; the solid collection angle, Ω_s, is usually set to 0.1 sr. In Ref. 5, considering the characteristics of a given Nd:YAG laser[58] and the example of HR measurements obtained by Pyatt and Shelton,[56] we show that the H_2-Ne CIHR spectra could be experimentally detected. As for the spectra of H_2-Kr and H_2-Xe CIHR, for which the signals are more intense, this conclusion can be applied as well. It is noteworthy that there is always a certain margin of adjustments of the experimental setup possible to enhance measuring performance. As it is to be shown, a proper choice of the scattering compound may be also applied to this effect.

IV. RESULTS AND FINAL REMARKS

The resulting values of the SA collisional hyperpolarizability components are presented in tables provided at http://zon8.physd.amu.edu.pl/~tbancewi. Figures 1–4 show the calculated profiles: the two heaviest colliding pairs are considered and compared, both in regard to the vector as well as the septor components of the hyperpolarizabilities. This allows analysis of characteristic features of the $\Delta\beta(R)$ dependence, of especially sophisticated nature within the small intermolecular distances. It should be reminded, however that also the monotonic low value tails are of essential importance for forming the central regions of the collisional HR lines, hence they also should be carefully studied. The discrete points in Figures 1–4 exemplify a few chosen sets of the *ab initio* method results. The lines represent functional dependence of the collisional hyperpolarizability on the intermolecular distance between H_2 and a noble gas scatterer are evaluated by applying the Marquadt-Levenberg fitting algorithm[59] (a modelling formula together with fitting parameters are available from the corresponding author upon request). The fitted functions are determined within a relatively wide range of separations ranging from R = 4 to 14 a_0 that, according to earlier assessments,[60] provides a satisfactory range for calculating reliable spectral shapes.

These spectral lines are depicted in Figures 5 and 6, where two representative examples of the overall R-T spectral profiles are shown: the vector type CI effect in H_2-Xe and the septor contribution in H_2-Kr mixtures both taken at room temperature of 295 K. The shapes are calculated mainly by means of the quantum-mechanical routines, yet the semiclassical points representing the total R-T contours (denoted "tot") are also marked for comparison. A nice agreement is observed between two data sets within the frequency domain that brings non-negligible contribution to the convolution of Eq. (2), i.e., not far than 360 cm^{-1} at the sides of the rotational peaks. In the logarithmic scale virtually no discrepancy between the QM and SC is visible. Even though more quantitative assessment reveals that the relative root mean square deviation of the QM and SC spectral lines reaches about 2.0% for the vector case and 2.5% for the septor-related results, this may anyway serve as a solid proof of the computational accuracy of the codes applied.

Partial profiles representing particular SA shares (marked 01, 03, 2X, and 4X in the figures) can be dissected from the overall theoretical spectrum so as to enable assessment various contribution to the detected signal. This is especially obvious for the *purely* translational profiles yielded by λL = 01 and 03 SA components, which participate mostly, albeit not exclusively, in shaping the central section of the R-T total spectrum (for ν between −200 and 200 cm^{-1}). On the other hand, the region of high frequency shift that begins at about 1800.0 cm^{-1} is almost solely determined by the total contribution corresponding to $\lambda = 4$ SA CIH (denoted by 4X). This section of the spectrum is partially related to the HR scattering with $\Delta J = \pm 4$, which accounts for its dominance over the remaining 01 and 2X shares in the wings of the R-T spectra in Figures 5 and 6. The $\lambda = 2$-related shape (2X) exhibits more meaningful presence for the frequency area spanning in between. Its role, however, cannot be as easily distinguished as these of previously mentioned parts.

Once the H_2-Kr and H_2-Xe are included into the spectral considerations a more comprehensive insight into the evolution of the role of the vector and septor part in forming the CIHR R-T shapes is possible. Analysis of this problem performed for the lighter scatterers[5,7] has revealed a dominance of the vector component in the low frequency region of the spectra ($|\nu| \leq 300$ cm^{-1}) and a predominant contribution of the septor part in the spectral wings. The light scattered on the heaviest pairs, however, has shown a growing influence of the latter component, which can be seen in Figures 8 and 9, where two graphs corresponding to the vector and septor parts of the depolarized intensity shapes are compared. This effect is especially visible in Figure 9, where additionally the two spectral components related to the least massive system, H_2-He, are plotted for comparison with the heaviest scatterer case of H_2-Xe. In both pictures the septor lines start to take precedence over the vector's share at $\nu \approx 1200$ cm^{-1} for H_2-Kr and $\nu \approx 500$ cm^{-1} for the heavier H_2-Xe compound. On the

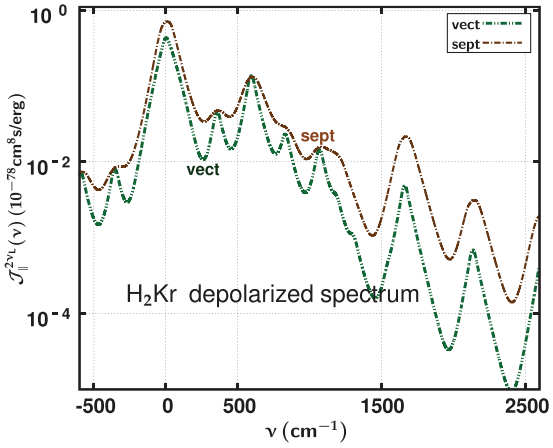

FIG. 8. Vector and septor parts of depolarized CIHR spectrum in H_2-Kr mixture.

one hand, this finding provides a partial proof of an increasing role of the short range collisional mechanisms (overlap, dispersion) with growing mass and size of scatterers, while on the other, it may deliver a clue in the efforts of designing an experimental method for discerning the hyperpolarizability component values of different order. To be more precise, the circumstance noted could hopefully enable numerical extraction of more reliable values of the vector and septor parts from measured polarized and depolarized HR signals.[8]

As far as the experimental prospects are considered, another kind of evolution in the total R-T spectral profiles can be observed. Namely, the spectral shapes demonstrated in Figure 7 can cast some light on the question of the experimental feasibility of the CIHR scattering measurements. In the picture the polarized spectral shapes corresponding to the Ne perturber are compared with the lines induced by the more polarizable, supermolecules including Kr and Xe atoms. The increase in the HR signal is noticeable and meaningful: the top spectral peak for the H_2-Xe scatterer is of about two orders of magnitude stronger than the relevant values for the hydrogen-neon case discussed in the section above; a similar increase, albeit to a lesser extent is apparent for H_2Kr. Bearing

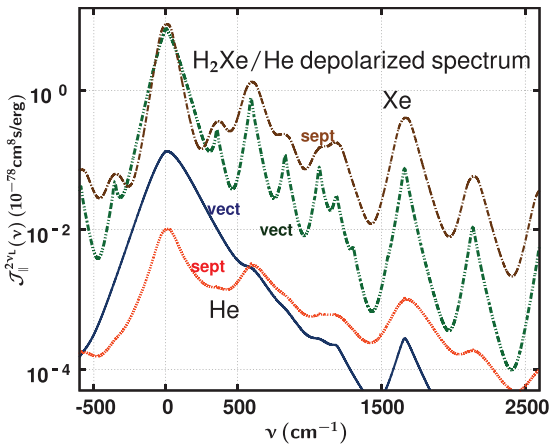

FIG. 9. Vector and septor parts of depolarized CIHR spectrum in H_2-Xe mixture. Additionally the same lines are given for H_2-He system for comparison (lines in bottom part of picture).

in mind that, according to Eq. (3) an experimentally detected CIHR signal expressed in the counts of photon per second is proportional to the calculated intensities, it may be expected that the obtained values should improve at approximately the same rate granting a better opportunity for reliable measurements.

As a result, the CIHR spectral properties have been analyzed with regard to the significance of the specific line shape components associated with irreducible tensorial quantities of particular order. Similarly to the previously considered processes in the mixtures of lighter colliding pairs, the dominant role of the purely translational $K\lambda L = 101$ and 303 lines has been found within the low frequency region. The influence of the septor related contributions, however, proves to be more pronounced for the H_2Kr and H_2Xe systems than in the earlier analyzed cases. The total intensities of the scattered signals are also meaningfully higher for these scatterers in comparison with their lighter counterparts. According to the analysis performed, the last two conclusions may be treated as a reliable incentive for prospective experimental efforts in the field of the nonlinear collisional light scattering phenomena.

ACKNOWLEDGMENTS

This paper has been supported by the research project Nr. N N202 069939 sponsored by The Polish Ministry of Sciences and Higher Education.

[1] J. E. Dove, A. C. M. Rusk, P. H. Cribb, and P. G. Martin, Astrophys. J. **318**, 379 (1987).
[2] *Molecular Complexes in Earth's Planetary, Cometary, and Interstellar Atmospheres*, edited by A. A. Vigasin and Z. Slanina (World Scientific, Singapore, 1998).
[3] L. Frommhold, *Collision-induced Absorption in Gases* (Cambridge University Press, Cambridge, 1993).
[4] X. Li, J. F. Harrison, M. Gustafsson, L. Frommhold, and K. L. C. Hunt, *Atomic and Molecular Nonlinear Optics: Theory, Experiment and Computation - A Homage to the Pioneering Work of Stanisław Kielich (1925–1993)*, edited by G. Maroulis, T. Bancewicz, B. Champagne, and A. D. Buckingham (IOS Press, Amsterdam, 2011), pp. 254–286.
[5] W. Głaz, J.-L. Godet, A. Haskopoulos, T. Bancewicz, and G. Maroulis, Phys. Rev. A **84**, 012503 (2011).
[6] L. Schlapbach and Z. Zuettel, Nature (London) **414**, 353 (2001).
[7] J.-L. Godet, T. Bancewicz, W. Głaz, G. Maroulis, and A. Haskopoulos, J. Chem. Phys. **131**, 204305 (2009).
[8] T. Bancewicz, W. Głaz, J.-L. Godet, and G. Maroulis, J. Chem. Phys. **129**, 124306 (2008).
[9] T. Bancewicz and G. Maroulis, Chem. Phys. Lett. **471**, 148 (2009).
[10] T. Bancewicz and G. Maroulis, Phys. Rev. A **79**, 042704 (2009).
[11] A. Haskopoulos and G. Maroulis, J. Phys. Chem. A **114**, 8730 (2010).
[12] W. Głaz, J. Comput. Methods Sci. Eng. **11**, 339 (2011).
[13] S. Kielich, Physica **30**, 1717 (1964).
[14] R. W. Terhune, P. D. Maker, and C. M. Savage, Phys. Rev. Lett. **14**, 681 (1965).
[15] P. D. Maker, Phys. Rev. A **1**, 923 (1970).
[16] D. A. Kleinman, Phys. Rev. **126**, 1977 (1962).
[17] J. Jerphagnon, D. Chemla, and R. Bonneville, Adv. Phys. **27**, 609 (1978).
[18] B. J. Berne and R. Pecora, *Dynamic Light Scattering* (John Wiley and Sons, New York, 1976).
[19] S. Kielich, J. R. Lalanne, and F. B. Martin, Phys. Rev. Lett. **26**, 1295 (1971).
[20] T. Bancewicz and Z. Ożgo, *Modern Nonlinear Optics*, Advances in Chemical Physics, Vol. 85, edited by M. Evans and S. Kielich (Wiley, New York, 1993), pp. 89–126.
[21] T. Bancewicz, Y. Le Duff, and J.-L. Godet, *Modern Nonlinear Optics, Part 1*, 2nd ed., Advances in Chemical Physics, Vol. 119, edited by M. Evans (John Wiley, New York, 2001), pp. 267–307.

[22]K. Clays, A. Persoons, and L. DeMayer, *Modern Nonlinear Optics*, Advances in Chemical Physics, Vol. 85(3), edited by M. Evans and S. Kielich (Wiley, New York, 1993), p. 455.
[23]F. Caset, E. Bogdan, A. Plaquet, L. Ducasse, B. Champagne, and V. Rodrigues, J. Chem. Phys. **136**, 024506 (2012), and references therein.
[24]D. P. Shelton, J. Chem. Phys. **137**, 044312 (2012), and references therein.
[25]J. M. Hartmann, C. Boulet, and D. Robert, *Collisional Effects on Molecular Spectra: Laboratory Experiments and Models, Consequences for Applications* (Elsevier, Amsterdam, 2008).
[26]P. Karamanis and C. Pouchan, Int. J. Quantum Chem. **111**, 788 (2011).
[27]A. K. Kudian and H. L. Welsh, Can. J. Phys. **49**, 230 (1971).
[28]A. R. W. McKellar and H. L. Welsh, J. Chem. Phys. **55**, 595 (1971).
[29]A. M. Dunker and R. G. Gordon, J. Chem. Phys. **68**, 700 (1978).
[30]M. Abu-Kharma, H. Y. Omari, N. Shawaqfeh, and C. Stamp, J. Mol. Spectrosc. **259**, 111 (2010).
[31]G. Maroulis, J. Phys. Chem. A **104**, 4772 (2000).
[32]G. Maroulis and A. Haskopoulos, Chem. Phys. Lett. **349**, 335 (2001).
[33]G. Maroulis and A. Haskopoulos, Chem. Phys. Lett. **358**, 64 (2002).
[34]S. Dixneuf, M. Chrysos, and F. Rachet, Phys. Rev. A **80**, 022703 (2009).
[35]G. Maroulis, A. Haskopoulos, and D. Xenides, Chem. Phys. Lett. **396**, 59 (2004).
[36]A. Haskopoulos, D. Xenides, and G. Maroulis, Chem. Phys. **309**, 271 (2005).
[37]S. Dixneuf, M. Chrysos, and F. Rachet, J. Chem. Phys. **131**, 074304 (2009).
[38]S. F. Boys and F. Bernardi, Mol. Phys. **19**, 553 (1970).
[39]J. E. Rice, P. R. Taylor, T. J. Lee, and J. Almloef, J. Chem. Phys. **94**, 4972 (1991).
[40]G. Maroulis and A. J. Thakkar, J. Chem. Phys. **89**, 7320 (1988).
[41]X. Li and K. L. C. Hunt, J. Chem. Phys. **100**, 7875 (1994).
[42] M. J. Frisch, G. W. Trucks, H. B. Schlegel *et al.*, GAUSSIAN 03, Revision D.01 (Gaussian, Inc., Wallingford, CT, 2004).
[43]U. Fano and G. Racah, *Irreducible Tensorial Sets* (Academic, New York, 1959).
[44]T. Bancewicz, Chem. Phys. Lett. **213**, 363 (1993).
[45]G. Maroulis, *Chemical Modelling: Applications and Theory*, Chem. Modell., Vol. 9, edited by M. Springbord (The Royal Society of Chemistry, Cambridge, 2012), pp. 25–60.
[46]A. Haskopoulos and G. Maroulis, private communication (2011).
[47]T. Bancewicz, J. Chem. Phys. **134**, 104309 (2011).
[48]W. Głaz, T. Bancewicz, J.-L. Godet, G. Maroulis, and A. Haskopoulos, Phys. Rev. A **73**, 042708 (2006).
[49]G. Maroulis, A. Haskopoulos, W. Głaz, T. Bancewicz, and J.-L. Godet, Chem. Phys. Lett. **428**, 28 (2006).
[50]W. Głaz, J. Yang, J. D. Poll, and C. G. Gray, Chem. Phys. Lett. **218**, 183 (1994).
[51]N. Meinander, J. Chem. Phys. **99**, 8654 (1993).
[52]H. Posch, Mol. Phys. **40**, 1137 (1980).
[53]H. Posch, Mol. Phys. **46**, 1213 (1982).
[54]R. J. L. Roy and J. M. Hutson, J. Chem. Phys. **86**, 837 (1987).
[55]H. Wei, R. J. L. Roy, R. Wheatley, and W. J. Meath, J. Chem. Phys. **122**, 084321 (2005).
[56]R. D. Pyatt and D. P. Shelton, J. Chem. Phys **114**, 9938 (2001).
[57]G. Boudebs and K. Fedus, J. Appl. Phys. **105**, 103106 (2009).
[58]J. M. Dawes and M. G. Sceats, Opt. Commun. **65**, 275 (1988).
[59]W. H. Press, S. A. Teukolsky, W. T. Vetterling, and B. P. Flannery, *Numerical Recipes* (Cambridge University Press, Cambridge, 1996).
[60]W. Głaz, *Proceedings of SPIE*, Vol. 8697 (SPIE, Bellingham, 2012), 869723.